Molecular Crystals and Liquid Crystals

ISSN: 1542-1406 (Print) 1563-5287 (Online) Journal homepage: http://www.tandfonline.com/loi/gmcl20

Study of Isothermal Crystallization Kinetics of 5CB with Differential Scanning Calorimetry and Broadband Dielectric Spectroscopy

D. Georgopoulos, S. Kripotou, E. Argyraki, A. Kyritsis & P. Pissis

To cite this article: D. Georgopoulos, S. Kripotou, E. Argyraki, A. Kyritsis & P. Pissis (2015) Study of Isothermal Crystallization Kinetics of 5CB with Differential Scanning Calorimetry and Broadband Dielectric Spectroscopy, Molecular Crystals and Liquid Crystals, 611:1, 197-207, DOI: 10.1080/15421406.2015.1030259

To link to this article: http://dx.doi.org/10.1080/15421406.2015.1030259

Mol. Cryst. Liq. Cryst., Vol. 611: pp. 197–207, 2015

ISSN: 1542-1406 print/1563-5287 online
DOI: 10.1080/15421406.2015.1030259

Taylor & Francis
Taylor & Francis Group

Study of Isothermal Crystallization Kinetics of 5CB with Differential Scanning Calorimetry and Broadband Dielectric Spectroscopy

D. GEORGOPOULOS,* S. KRIPOTOU, E. ARGYRAKI, A. KYRITSIS, AND P. PISSIS

National Technical University of Athens, Department of Physics, Athens, Greece

The isothermal crystallization kinetics of 4-n-pentyl-4–cyanobiphenyl (5CB) has been studied with Differential Scanning Calorimetry (DSC) and Dielectric Relaxation Spectroscopy (DRS). 5CB is a well characterized material which makes it ideal for a dielectric and thermal comparative study. The effect that isothermal crystallization exerts on the behavior of relaxation processes α and δ by cooling the isotropic liquid below the nematic phase or through the process of cold crystallization by heating it from the supercooled state is explored by comparing the DRS and DSC. Furthermore, by employing the Avrami equation, we compare the ability to probe the crystallization with each technique.

Keywords 5CB; crystallization; DRS; DSC; Avrami

Introduction

What change the crystallization induces on the relaxation processes of a glass forming material is a fundamental question which is yet to be fully answered. In order to address this problem properly, it is necessary to have knowledge both of the crystallization process and the segmental dynamics. The most common method for studying the crystallization kinetics is differential scanning calorimetry (DSC) [1, 2] either isothermally or even non-isothermally [3], while broadband dielectric relaxation spectroscopy (DRS) is one of the main techniques for studying molecular dynamics [4–9]. So, by combining these two different approaches we may obtain a much more comprehensive view of the relation between molecular mobility and structural changes.

In the past, there have been several studies on polymers [10–15] where both techniques were applied with the purpose of investigating the evolution of the main α relaxation process over time at a constant temperature where crystallization occurs. However, establishing a general connection between the fraction of crystallinity (X_c) and molecular mobility by just comparing the dielectric spectra with calorimetric data is rather impossible. There were cases like in Poly(trimethylene terephthalate) [10] or Poly(ether ether ketone) [11], where the main α relaxation process shifted to lower frequencies with the reduction of the amorphous fraction at a fixed temperature, became faster like in Poly(L-lactic acid) [12] or portrayed an even more complex behavior like the one observed in Poly(dimethylsiloxane)

*Address correspondence to D. Georgopoulos, National Technical University of Athens, Department of Physics, Zografou Campus 15780, Athens, Greece; E-mail: dimosgeo@central.ntua.gr

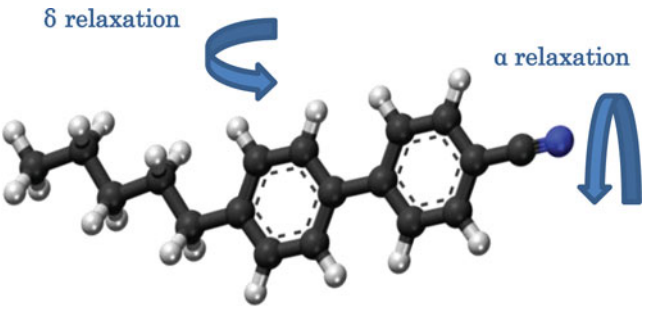

Figure 1. The molecular structure of 4-n-pentyl-4–cyanobiphenyl (5CB).

[13] or by C. Alvarez et al. in Poly(ethylene terephthalate)[14]. Furthermore, one must consider not only the complexity of the molecule, but also the crystallization process itself especially in cases of materials that exhibit polymorphism, where the thermal treatment defines the type of the crystal structure that will be created.

In the present work we employ differential scanning calorimetry and dielectric relaxation spectroscopy to investigate the connection between the development of the crystallization process and the dielectric behavior of 4-n-pentyl-4–cyanobiphenyl (5CB). The calamitic 5CB is one of the most fundamental liquid crystals which makes it an ideal system for this type of study, since it has well characterized phase transitions [16–18] and relaxation processes [7,19–22]. Thermally, it exhibits isotropic, nematic and solid phase where the material is either amorphous or crystallized, with transition temperatures around 35°C ($T_{I\text{-}N}$) and 20°C ($T_{N\text{-}S}$) and a glass transition temperature at about −70°C [18] in amorphous phase. Moreover, for its crystal structure, Moura Ramos et al. [18] have found that 5CB shows two different crystal polymorphs depending on whether the material is crystallized by being cooled to just below the nematic phase from the molten state (polymorph 1) or heated from the supercooled nematic phase (polymorph 2). Dielectrically, 5CB features a dipole moment along the long axis, that exhibits two relaxation processes, the slow δ process and the faster α process, which are connected with the rotations around its center of mass as depicted in Fig 1 [7, 20, 23].

Here, we follow molecular mobility with DRS during isothermal cold crystallization by heating it from the supercooled nematic phase (−120°C) to −52°C (experiment A) and during isothermal crystallization of the sample by cooling it from the isotropic phase to −15°C (experiment B). During cold crystallization at −52°C, both relaxation processes can be observed within the frequency window of our technique, while for the isothermal crystallization at −15°C (experiment B) only the slower, δ relaxation, can be dielectrically recorded. Moreover, for the analysis of the crystallization process we use the model proposed by M. Avrami [24, 25] and the well-known equation:

$$\varphi_c = 1 - e^{-k(t-t_0)^n} \tag{1}$$

where φ_c is the relative crystallinity, k is a temperature dependent isothermal crystallization rate constant, τ_0 is the time at which the crystallization begins, and n is the Avrami index from which we can extract information about the development of the crystal structure.

To the best of our knowledge, no study of 5CB has tackled with the effect that crystallization exerts on the segmental dynamics with comparative DRS and DSC measurements. In the present study, we further explore the connection of dielectric strength, shape and position of the relaxation mechanisms with the proportion of crystallinity. In addition, we examine the divergence of the method used to probe the crystallization kinetics by employing solely dielectric measurements [26, 27] with the results that we get from calorimetry.

Experimental

The 5CB compound was commercially available by Merc and it was used without further processing. For the DRS measurements a single drop of the sample was introduced between two brass electrodes (15mm diameter) with a micro syringe, which did not undergo any special treatment in order to avoid any induced orientation to the interfacial molecules. The distance between the plates of the capacitor was fixed at 50 μm with the use of silica spacers. The equipment used for the dielectric measurements was a Novocontrol Alpha Analyzer in combination with a Novocontrol Quatro Cryosystem (temperature stability better than $\pm 0.1^{\circ}$C).

Two different experimental protocols were followed for 5CB, one for studying the cold crystallization at -52°C (experiment A) and one for the crystallization by cooling it from the isotropic phase to -15°C (experiment B). The selection of these crystallization temperatures was based on having the optimal image of the relaxation processes which is necessary for the dielectric analysis.

If the liquid crystal is cooled down from the isotropic phase at cooling rates higher than 2–3°C/min, the material can easily get to the amorphous phase and then it crystallizes during heating, while for slower cooling rates it crystallizes below the temperature of the nematic-solid phase transition. So, in order to study the cold crystallization (experiment A), firstly, the sample was heated to the isotropic phase (60°C) and then it was cooled down to -120°C with a sufficiently high temperature rate of 10°C/min, in order to avoid crystallization and get the 5CB in the glassy state. Subsequently, the liquid crystal was heated with a rate of 5°C/min and stabilized at -52°C, where successive sweeps of the dielectric function (10^0–10^6 Hz) were made with a time interval of 200 s in order to follow the relaxation processes during the cold crystallization.

An analogous protocol was followed for probing the crystallization at -15°C (experiment B). The sample was initially heated up to the isotropic phase (60°C) and then cooled down to -15°C with a rate of 5°C/min in order to avoid crystallization prior to the temperature stabilization. Having stabilized the temperature at -15°C, isothermal scans of the dielectric spectra were made in the frequency window 10^3–10^6 Hz every 75 s, in order to follow the δ relaxation during the phase transition. Furthermore, with the same thermal protocol, the signal at specific frequencies (10,70, and 100 kHz) was recorded every 15 s in order to compare divergence from the full dielectric spectrum.

The same experimental protocols to the ones mentioned above were used for the DSC measurements to record the crystallization at -52°C and -15°C, in order to enable direct comparison with the recorded DRS results. The equipment used was Q200 of TA Instruments and the sample (4–5 mg) was sealed in a Tzero hermetic pan and measured in helium atmosphere.

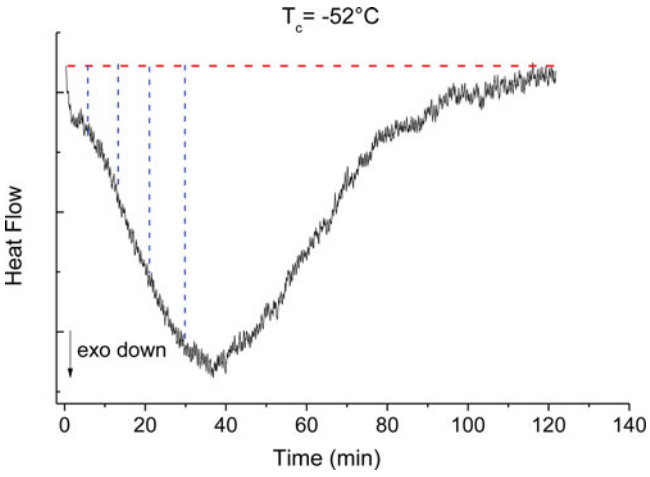

Figure 2. Heat flow as a function of time during the cold crystallization of 5CB at $T_c = -52^{\circ}C$. The dashed lines describe the integration process followed for the calculation of the crystallinity's time dependency.

Results and Discussion

DSC Results

The analysis of the DSC data was conducted according to the guidelines provided in [28] for the isothermal cold crystallization at $-52^{\circ}C$ (experiment A) and the crystallization by cooling the sample from the isotropic phase to $-15^{\circ}C$ (experiment B). However, since there is no standard ΔH value for fully crystallized 5CB, for the calculation of the amorphous fraction it was assumed for both crystallization experiments that the recorded exothermic peak describes the transition from a fully amorphous material to a fully crystallized. Therefore, the function of crystallinity (X_c) versus time was calculated by dividing and adding the time based slices with the whole integral as shown in Fig. 2 for the isothermal crystallization at $-52^{\circ}C$ (experiment A). Nevertheless, this assumption may not be completely accurate in the case of the cold crystallization experiment since during the cooling of the sample, crystallization might have not been completely avoided, even though it was not clearly recorded with DSC. Furthermore, the crystal fraction versus time for both crystallization temperatures is presented in Fig. 3, where we can clearly observe the difference in the time needed for the completion of the transition between the slowly developing cold crystallization at $-52^{\circ}C$ and the faster one at $-15^{\circ}C$.

Molecular Mobility and Crystallization

Figure 4 shows the imaginary and real part of dielectric function from consecutive frequency sweeps during isothermal cold crystallization of 5CB at $-52^{\circ}C$ (experiment A). By being in the supercooled nematic state, both the α and δ relaxation processes are well established within the frequency window (10^0–10^6 Hz) of our experimental equipment at $-52^{\circ}C$, where the cold crystallization occurs, in accordance with a previous work [16]. At this temperature, the progress of crystallization is slow enough, so that the changes of crystallinity can be

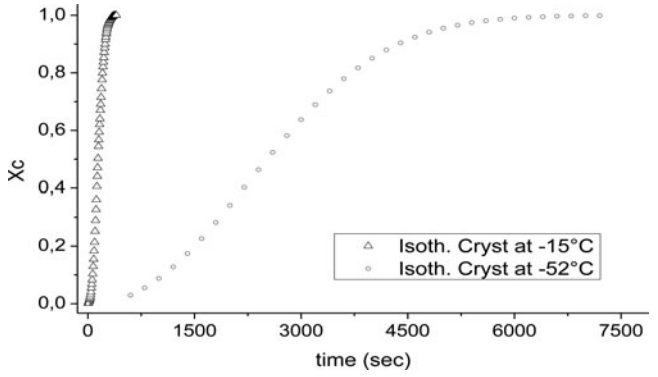

Figure 3. The crystal fraction (X_c) versus time for isothermal crystallization at -52°C (circles) and -15°C (triangles).

neglected during the time needed for the completion of frequency sweep and that the relaxation mechanisms' shape is undistorted.

From the $\varepsilon'(f)$ in Figure 4 (b) a clear peak can be observed at about 20 Hz that corresponds to δ relaxation and one not so clear located close to 1 kHz of the α relaxation. The experimental results of dielectric losses are fitted with the Havriliak-Negami equation [30,31]:

$$\varepsilon''(\omega) = \sum_{k=1}^{2} \left(\frac{\Delta\varepsilon}{\left[1 + \left(i\omega \frac{f}{f_{HN,k}}\right)^{\alpha_k}\right]^{\beta_k}} \right) \tag{2}$$

where $\Delta\varepsilon$ denotes the dielectric strength of the relaxation, α and β describe the symmetric and asymmetric broadening of the peak ($\alpha = \beta = 1$ for Debye) and f_{HN} is related to the frequency of the peak f_{max} ($f_{HN} = f_{max}$ when $\beta = 1$).

As the time lapses and the crystallization progress, the intensity of both relaxation processes decreases while their position remain unaffected. A more thorough analysis

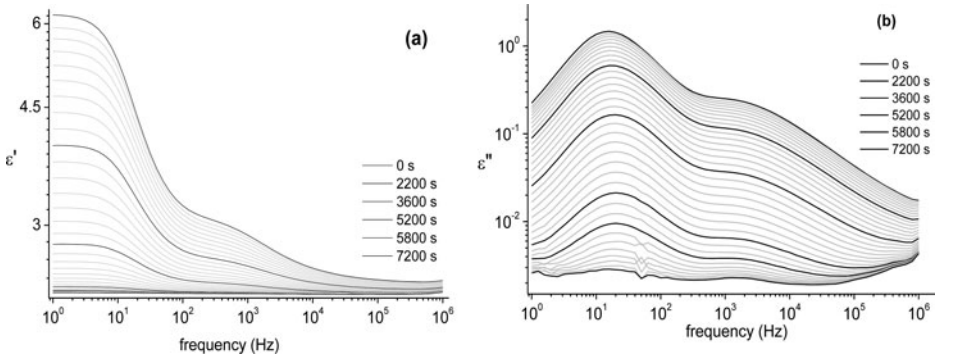

Figure 4. Real and imaginary part of dielectric function, ε' and ε'', as a function of frequency in a and b, respectively, at different time moments for 5CB during isothermal crystallization at $Tc = -52^{\circ}$C.

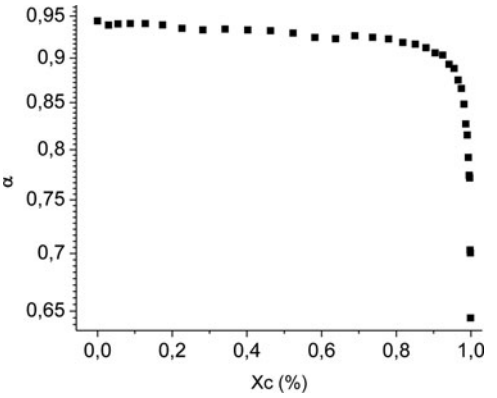

Figure 5. The α shape parameter of the δ relaxation as a function of time for 5CB during isothermal crystallization at $T_c = -52^{\circ}C$

of the above data is accomplished by the application of eq. 2. Fitting the data with the H-N equation shows that the δ relaxation is almost completely symmetrical ($\beta \approx 1$) and progressively broadens as the crystallinity increases. In Fig. 5 the α-shape parameter of δ relaxation is plotted versus the crystal fraction (X_c) from DSC measurements, where we can see a steady decrease of the symmetric broadening parameter until we reach high crystallinity and the decrease becomes sharp.

However, in the case of the α relaxation the analysis was hindered due to the close proximity of the two relaxation processes and the existence of a faster component which becomes clearly visible as the crystallization progresses and the dielectric strength of the main relaxation processes diminishes. This faster process was observed in a previous work [16] and it affects the accuracy of the data fitting for the α relaxation as the crystallization progresses, especially for time t > 5800 s. In order to fit the α relaxation, for the slope at the high frequency wing that is described by the Jonscher [31] relation:

$$\frac{\varepsilon\left(f > f_{peak}\right)}{\varepsilon_{peak}} \propto \left(\frac{f}{f_{peak}}\right)^{-n} \tag{3}$$

the value of n, which is correlated with the H-N coefficient $n = \alpha \cdot \beta$, was kept at 0.5. The value of this parameter was close to the mean value derived from freely fitting the H-N eq. and it was selected also in accordance with the one proposed by Olsen et al.[32] for glass forming systems close to glass transition temperature (T_g) since $\left|T_g - |T_c|\right| \cong 20^{\circ C,}$ and the analysis done by A. Drozd-Rzoska [33]. Alternatively, the α relaxation could be clearly studied in a confined system [7], where δ would be suppressed, which, however, would affect the crystallization.

By applying the above fitting procedure, the relative dielectric strength ($\Delta\varepsilon_{(t)}/\Delta\varepsilon_{(t=0)}$) of the α and δ relaxation as a function of time is presented in Fig. 6. Even though both molecular motions derive from the same amorphous fraction we can observe from Fig. 6 that the slower δ relaxation seems to be slightly more obstructed than the α relaxation which could be attributed to the fact that it is a larger scale motion.

For the isothermal crystallization at $-15^{\circ}C$ (experiment B), the ε' and ε" of the dielectric function at different time moments are shown in Fig. 7(a) and (b), respectively the peak presented in the dielectric losses of fig 7(b) corresponds to the slower δ mechanism,

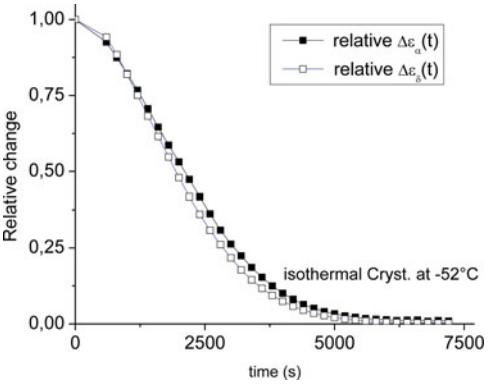

Figure 6. The relative change in the dielectric strength of the α and δ relaxation as function of time.

while the α relaxation at this temperature is located at higher frequencies which are beyond our frequency window. Contrary to the cold crystallization experiment, the transition to the crystalline phase, at $T_c = -15°C$, is much faster (Fig 3) and, as a result, the sample is in a different state at the beginning and at the end of a frequency sweep, even though the measurement's range is limited between 1 kHz and 1 MHz. This is the reason for the decrease in ε' at low frequencies in Fig. 7 (a) and the distorted shape of the peaks in ε". Because of this it is impossible to get reliable results by fitting the H-N equation in order to study the changes of the shape parameters or the dielectric strength as the crystallization takes place.

Crystallization Kinetics: DSC Vs DRS

Before directly comparing the DSC and the DRS technique as means of studying the crystallization kinetics we should review how each one of them records the transition in order to understand the divergence between them. Firstly, the basis for the differential scanning calorimetry is to simply record latent heat released during the transition to the crystal phase. However, instead of just considering the proper parameters of the experiment

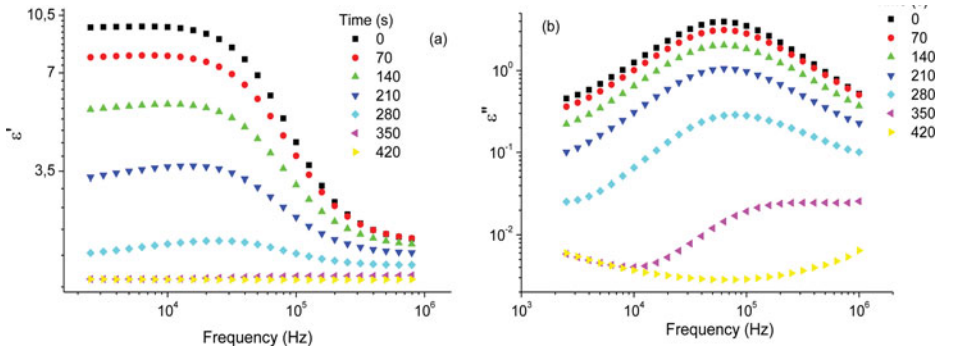

Figure 7. Imaginary and real part of dielectric function, ε' and ε", as a function of frequency in a and b, respectively, at different time moments for 5CB during isothermal crystallization at $Tc = -15°C$. The depicted peak at ε" (b) corresponds to δ relaxation.

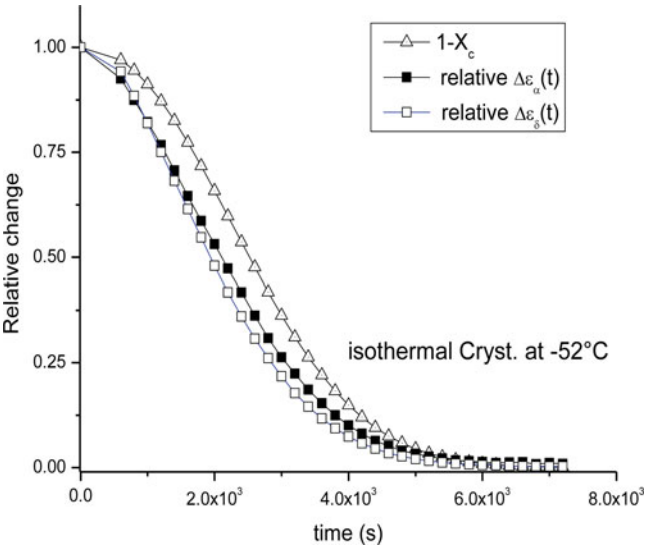

Figure 8. The relative dielectric strength of the α, δ relaxation (squares) from the DRS measurements and the amorphous fraction (triangles) from DSC vs time at -52°C

like thermal treatment, cooling rates etc. [28], it is important to consider heat transfer effects due to sample size as reported in [34] or distortion of the crystallization kinetics from the released heat [35], which, especially in cases of materials with low thermal conductivity, is significant for the proper analysis of the crystallization process.

On the other hand, the function of dielectric relaxation spectroscopy could be simplified as the recording of the response to an external field which is analogous to the population of the mobile "units" of the material. Therefore, in contrast to DSC, it is unaffected from problems mentioned above and, even more, small changes of non-homogenous temperature in the sample can be detected from the drift of the relaxation peak, if the accuracy of the temperature stabilization of the sample is high enough. Nevertheless, it cannot be considered the sole tool for such a study, since most of the materials deviate from being ideal and, therefore, either the quality of the signal or more complex parameters, like interfacial mechanisms, the parallel or antiparallel orientation of the dipole moments etc., make it rather complicated.

Having briefly commented on the basic principles and drawbacks of each technique, the transition of the supercooled sample to the crystal phase over time at -52°C (experiment A) is shown in Fig. 8, as it was recorded by both techniques. From Fig. 8 n, the DSC technique appears to have a hysteresis compared to the DRS in recording the transition and, in particular, $\Delta\varepsilon$ decreases faster than $1-X_c$ in the initial stages of crystallization, which could be attributed to the ability of the latter to record even the formation of nuclei which cannot be detected with calorimetry. Moreover, by associating the relative dielectric strength of the relaxation processes with corresponding DSC results we get from Fig. 9 directly the relation of the $\Delta\varepsilon/\Delta\varepsilon_{(xc=0)}$ with the calorimetric amorphous fraction. We can clearly observe in figure 9 that the relation between the two quantities diverges from being completely linear in the whole region.

In the case of the isothermal crystallization at -15°C (experiment B), the fast development of the crystal phase made impossible the exploitation of the dielectric spectra

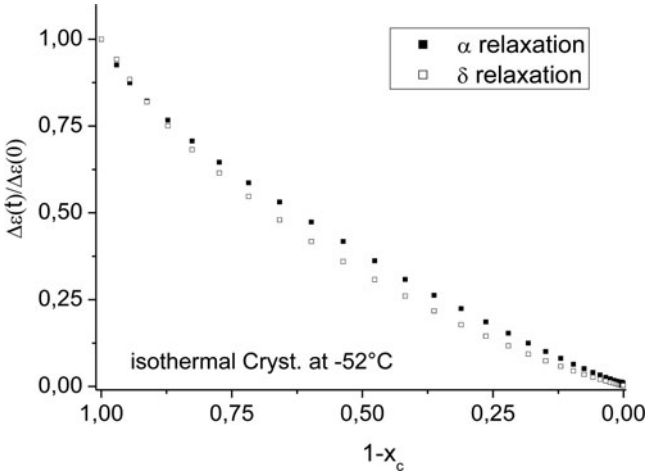

Figure 9. The relative dielectric strength of the α and δ relaxation from DRS as a function of the amorphous fraction from DSC during isothermal crystallization at -52°C

by fitting the H-N model and consequently probing the transition in comparison with the DSC. For this reason, instead of a frequency window sweep, the dielectric response at three specific frequencies (10 kHz,70 kHz, and 100 kHz) was recorded, similar to previous studies [26,27], and will be discussed below in accordance with the Avrami model [24,25].

In order to further explore the difference in following the crystallization process we employ the Avrami model. For the DSC data the application of equation 1 is adequate, while for the DRS results it should be modified as in [26,27] on the basis that $\Delta\varepsilon$ is proportional to the amorphous fraction:

$$\frac{\Delta\varepsilon(t)}{\Delta\varepsilon(0)} = \frac{\varepsilon'_{\alpha}(f,t) - \varepsilon'_{\infty}}{\varepsilon'_{\alpha}(f,0) - \varepsilon'_{\infty}} = \frac{\varepsilon_{\alpha}(f,t)}{\varepsilon_{\alpha}(f,0)} = exp\left[-\left(k \cdot t^{m}\right)\right] \tag{4}$$

where the parameters k and m express the same meaning as in eq. (1). In the case of a full spectrum, the used $\Delta\varepsilon$ calculated by fitting the H-N is used, whereas for fast developing transitions, the measured ε' and ε' at specific frequency f over time t are used.

The Avrami plots of the dielectric and the calorimetric data for both crystallization temperatures (experiments A and B) are presented in Fig. 10 (a) and (b). For the cold crystallization at -52°C in Figs. 10(a) (experiment A) the calculated Avrami index from linear fitting is about 1.8 and 2.1 for DRS and DSC results, respectively. For the crystallization by cooling from the isotropic phase at -15°C in fig 10(b) (experiment B), on the other hand, the calculated values of n are 1.9 from the dielectric and 2.3 from the calorimetric data. Firstly, the differences in following the crystallization, between the two techniques, are insignificant, especially if we consider factors like the accuracy of the temperature stabilization of each device or the time that lapses until the stabilization is achieved. Moreover, the relative difference of n between the isothermal crystallization at -52°C and -15°C is adequate small, so that we may suggest that the development process of the crystal structure is same in both cases even though we have two different polymorphs at these two temperatures. However, a similar behavior has also been observed previously in a study of the transition between different crystalline phases of liquid-crystal mesogen 4,4′-di-n-butyloxyazoxybenzene (4-OAOB) [36]. Finally, for further analysis of the above

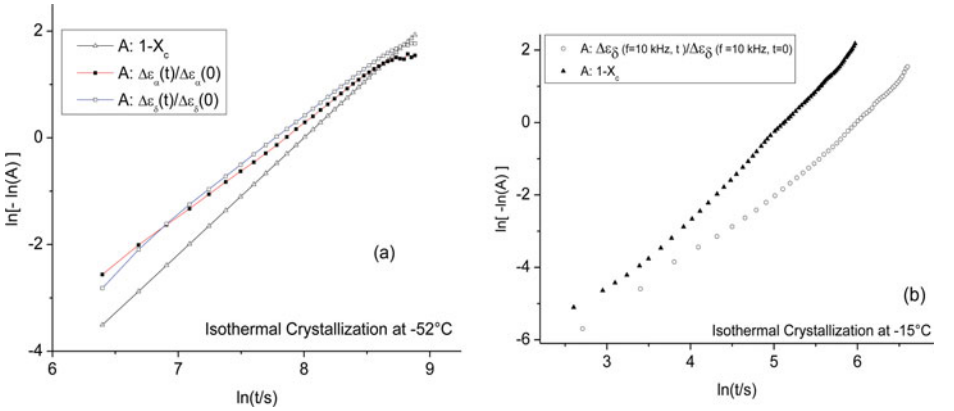

Figure 10. The linear form of the Avrami plots of the dielectric and calorimetric data for isothermal crystallization at -52°C (a) and at -15°C(b)

calculated values it would be essential to probe the crystallization with polarized optical microscopy, which was outside the frame of the current study.

Conclusions

The effect of the crystallization on the molecular dynamics of the liquid crystal 4-n-pentyl-4'-cyanobiphenyl (5CB) was investigated by broadband dielectric relaxation spectroscopy (DRS) and differential scanning calorimetry (DSC). The changes of the α and δ relaxation were probed during isothermal crystallization at two different temperatures in order to have different crystal structure (polymorphs). In the case of the slow evolving cold crystallization experiment at -52°C, the use of adequately wide frequency sweeps enabled the analysis of the α and δ mechanisms in terms of dielectric strength and shape by fitting model functions to the data, while in the case of faster crystallization at -15°C the produced dielectric data from frequency sweeps were unsuitable for reliable analysis.

Moreover, in the present study, the DRS and the DSC technique were compared as means of monitoring the transition to the crystal phase. Based on the function principles of each method, we further explored the resolution of each technique at the same experimental conditions and divergence between them by employing the Avrami model. Addition of polarized light microscopy as a third complementary technique for monitoring crystallization in future work may shed further light on these issues.

Funding

This research has been co-financed by the European Union (European Social Fund, ESF) and Greek national funds through the Operational Program "Education and Lifelong Learning" of the National Strategic Reference Framework (NSRF), Research Funding Program: THALES.

Acknowledgment

The authors are grateful to Dr. Daniel Fragiadakis for providing the analysis program Grafity (http://grafitylabs.com/).

References

[1] Godwosky, Y. K., & Slonimsky, G. L., (1974). *J. Polym. Sci. Polym. Phys.*, *12*, 1053.
[2] Kamal, M. R., Chu, E., (1983). *Polym. Eng., Sci.*, *23*, 27–31.
[3] Ozawa, T., (2001). *J. Therm. Anal. Calorim.*, *64*, 109–126.
[4] Moscicki, J. K. (1992). In: *Liquid Crystal Polymers: From Structures to Applications*, Collyer, A. A. (Ed.), Chapter 4, Elsevier: London, 143.
[5] Williams, G. (1993). In: *Materials Science & Technology Series*, Thomas, E. L. (Ed.), VCH Publications: Weinheim, Vol. 12, 471.
[6] Simon, G. P. (1997). In: *Dielectric Spctroscopy of Polymeric Materials: Fundamentals and Applications*, Runt, J. P. & Fitzgerald, J. J. (Eds.), Chapter 12, American Chemical Society: Washington, DC, 329.
[7] Kremer, F. & Schoenhals, A. (2003). In: *Broadband Dielectric Spectroscopy*, Kremer, F. & Schoenhals, A. (Eds.), Chapter 10, Springer: Berlin, 385.
[8] Nordio, P. L., Rigatti, G. & Segre, U. (1973). *Mol. Phys.*, *25*, 129.
[9] Williams, G. (1994). In: *The Molecular Dynamics of Liquid Crystals*, Luckhurst, G. R. & Veracini, C. A. (Eds.), Chapter 17, Kluwer Academic: Dordrecht, 431.
[10] Sanz, A., Nogales, A., Ezquerra, T. A., Soccio, M., Munari, A., Lotti, N., (2010). *Macromolecules*, *43*, 671
[11] Nogales, A., Ezquerra, T. A., Denchev, Z., Šics, I., Baltá Calleja, F. J., Hsiao, B. S., (2001). *J. Chem. Phys.*, *115*, 3804.
[12] Bra, A. R., Malik, P., Dionısio, M., Mano, J. F., (2008). *Macromolecules*, *41*, 6419
[13] Lund, R., Alegria, A., Goitandia, L.,(2008). *Macromolecules*, *41*, 1364
[14] Alvarez, C. *et al.*, (2004). *Polymer*, *45*, 3953.
[15] Mijovic, J. & Sy, J.,(2002). 6370–6376 (2002).
[16] Kripotou, S., Georgopoulos, D., Kyritsis, A. & Pissis, P., (2015). *Mol. Cryst. Liq. Cryst*
[17] Bonvalet, G. A., (1999). "Differential Scanning Calorimetric Study of the Nematic Liquid Crystal 5CB", Physics Department, The College of Wooster,
[18] Moura Ramos, J. J. & Diogo, H. P. (2013). *Mol. Cryst. Liq. Cryst.*, *571*, 19.
[19] Zeller, R., (1982). *Phys. Rev. Lett.*, *48*, 334.
[20] Aliev, F. M., Bengoechea, M. R., Gao, C. Y., Cochran, H. D., Dai, S., (2005). *J. Non. Cryst. Solids*, *351*, 2690.
[21] Drozd-Rzoska, A., (2009). *J. Chem. Phys.*, *130*, 234910.
[22] Belyaev, B. A., Drokin, N. A., Shabanov, V., (2005). *Phys. Solid State*, *47*, 765.
[23] Rozanski, S., Kremer, F., Groothues, H., Stannarius, R., (1997). *Mol. Cryst. Liq. Cryst.*, *303*, 319–324
[24] Piorkowska, E., Galeski, A., Haudin, J.-M., (2006). *Prog. Polym. Sci.*, *31*, 549.
[25] Avrami, M., (1939). *J. Chem. Phys.*, *7*, 1103.
[26] Avrami, M., (1940). *J. Chem. Phys.*, *8*, 212.
[27] Mohan, M., (2010). *Rom. J. Phys.*, *55*, 360.
[28] Massalska-Arodz, M., Williams, G., Smith, I. K., Conolly, C., Aldridge, G. A., and Dabrowski, R., (1998). *J. Chem. Soc. Faraday Trans.*, *94*, 387.
[29] Lorenzo, T., Arnal, M. L., Albuerne, J., and Müller, A. J., (2007). *Polym. Test.*, *26*, 222.
[30] Havriliak, S., Negami S., (1966). *J. Polym. Sci. C*, *16*, 99.
[31] Havriliak, S., Negami, S., (1967). *Polymer*, *8*, 161.
[32] Jonscher, A. K., (1977). *Nature*, *267*, 673.
[33] Olsen, N. B., Christensen, T. & Dyre, J. C., (2001). *Phys. Rev. Lett.*, *86*, 1271.
[34] Drozd-Rzoska, A., Rzoska, S., Pawlus, S. & Zioło., (2005). *Phys. Rev. E*, *72*, 031501
[35] Hargis, M. J. ,& Grady, B. P., (2006). *Thermochim. Acta*, *443*, 147.
[36] Piorkowska, E., (1997). *j. Appl. Polym. Sci.*, *66*, 1015.
[37] Bamezai, R. K., Godlewska, M., Massalska-Arodź, M., Ściesiński, J. and Witko, W., (1990). *Phase Transitions*, *27*, 113.